

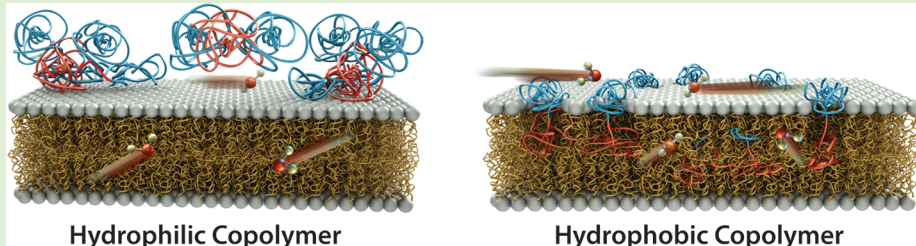
Nature of Interactions between PEO-PPO-PEO Triblock Copolymers and Lipid Membranes: (II) Role of Hydration Dynamics Revealed by Dynamic Nuclear Polarization

Chi-Yuan Cheng,^{†,‡} Jia-Yu Wang,^{†,§} Ravinath Kausik,^{‡,||} Ka Yee C. Lee,^{*,§} and Songi Han^{*,‡}

[†]Department of Chemistry and Biochemistry, University of California, Santa Barbara, California 93106, United States

[§]Department of Chemistry, Institute for Biophysical Dynamics and James Franck Institute, University of Chicago, Chicago, Illinois 60637, United States

^{||}Schlumberger-Doll Research, Cambridge, Massachusetts 02139, United States



ABSTRACT: Amphiphilic poly(ethylene oxide)-poly(propylene oxide)-poly(ethylene oxide) copolymers, also known as poloxamers, have broad biomembrane activities. To illustrate the nature of these activities, ¹H Overhauser dynamic nuclear polarization NMR spectroscopy was employed to sensitively detect polymer–lipid membrane interactions through the modulation of local hydration dynamics in lipid membranes. Our study shows P188, the most hydrophilic poloxamer that is a known membrane sealant, weakly adsorbs on the membrane surface, yet effectively retards membrane hydration dynamics. Contrarily, P181, the most hydrophobic poloxamer that is a known membrane permeabilizer, initially embeds at lipid headgroups and enhances intrabilayer water diffusivity. Unprecedented resolution for differentiating weak surface adsorption versus translocation of polymers to membranes is obtained by probing local water diffusivity in lipid bilayer systems. Our results illustrate that the relative hydrophilic/hydrophobic ratio of the polymer dictates its functions. These findings gleaned from local hydration dynamics are well supported by a thermodynamics study presented in the accompanying paper (Wang, J.-Y.; Marks, J. M.; Lee, K. Y. C. *Biomacromolecules*, 2012, DOI: 10.1021/bm300847x).

1. INTRODUCTION

As an efficient barrier between different biological compartments, the cell membrane is an active interface for the exchanges of energy, materials, and signals. For this purpose, the lipid membrane appears to be a dynamic platform where diverse biological functions occur through interactions between the membrane and various biomolecules. For instance, structurally compromised cell membranes induced by trauma, injuries, or diseases can be restored by interactions with a series of poly(ethylene oxide) (PEO)-based polymers,^{1–4} such as poloxamers, poloxamines, and polyethylene glycol (PEG) homopolymers. Poloxamers and poloxamines are a class of surface active amphiphilic copolymers composed of hydrophilic PEO and hydrophobic poly(propylene oxide) (PPO) blocks. The former is a linear PEO-PPO-PEO triblock copolymer; the latter is a four-armed PEO-PPO block copolymer joined by an ethylene diamine (see Chart 1). It has been found that the most hydrophilic poloxamer P188 is effective in treating acute heart failure and necrosis of muscle cells by restoring the structural integrity of damaged cell membranes.^{2–4} The most hydrophobic poloxamer P181, on the other hand, has been reported

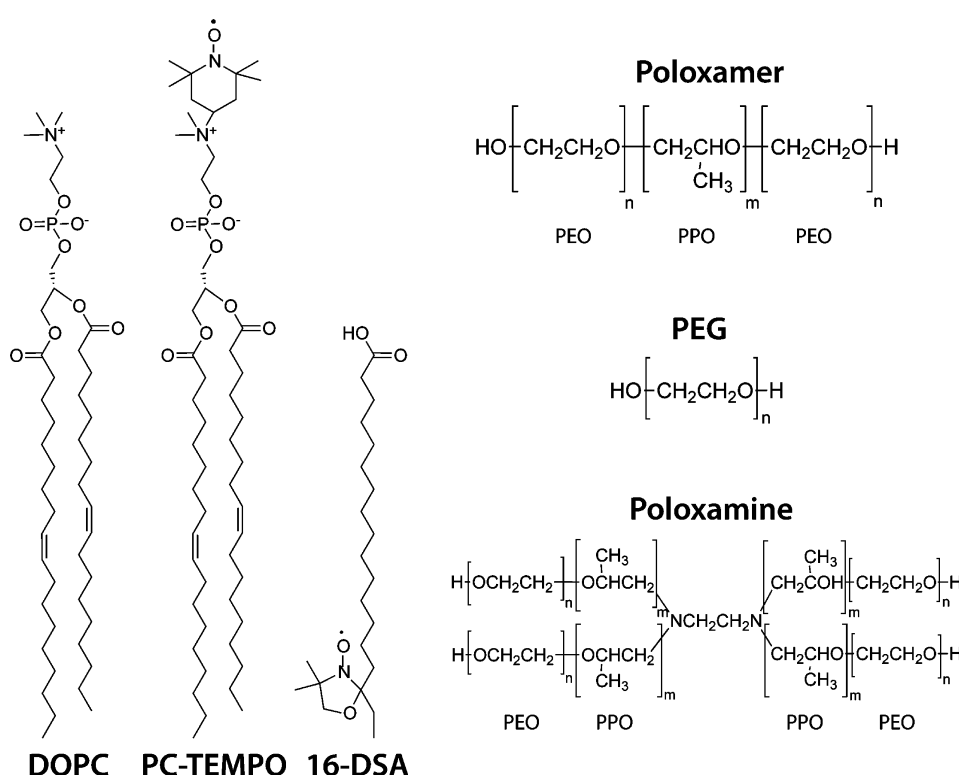
as a membrane permeabilizer that can facilitate the passage of molecules across lipid membranes.^{5,6} Biomedical applications of these two copolymers are of eminent interest; however, their implementations are empirically determined, given the technical challenges of unraveling their inherently weak interactions with lipid membranes under physiological conditions. Although several established techniques can provide dynamics and thermodynamics information of interactions between lipid membranes and biomacromolecules,^{7–10} they are typically insensitive to the interactions involving such weak bindings, especially those that do not involve measurable changes in the structure or dynamics of the participating macromolecules. Therefore, an alternative and more sensitive analytical tool will be highly desirable.

Following the preceding paper,¹ here we exploit interactions between the two polymers, P188 and P181, and lipid membranes through the modulation of membrane *hydration dynamics* induced by molecular interactions, using our newly

Received: May 31, 2012

Published: July 18, 2012

Chart 1. Chemical Structures of the DOPC Lipid, Spin-Labels of PC-TEMPO and 16-DSA, Poloxamer, Poloxamine, and PEG Homopolymer



developed technique, ^1H Overhauser dynamic nuclear polarization (ODNP) enhanced NMR spectroscopy.^{11–13} We chose local diffusion dynamics of loosely bound hydration water as our probe, because it composes an active and sensitively responsive matrix at the interface of biomembranes. It is now well-accepted that water at (bio)macromolecular interfaces and assemblies is dramatically implicated in a range of biochemical processes, including the stabilization of cell membranes,¹⁴ protein folding,^{15,16} early protein aggregation events,¹⁷ and the activation of transport proteins.¹⁸ Its nature and role in these biological systems and processes, however, are mainly provided or proposed by theoretical studies.^{19–21} While a few experimental approaches are available for mapping out hydration dynamics in biological systems, they all require particular sample conditions that are either incapable of offering site-specificity for measuring local hydration dynamics^{22–27} or unamenable to lipid membrane systems.^{25–28} The basic idea behind our new analytical strategy is to probe the interactions between these poloxamers and lipid vesicles by exploiting the delicate modulation of the translational diffusion dynamics of the relatively thick (10–20 Å) hydration layers,¹⁶ typically termed loosely bound or outer sphere water, both on the lipid membrane surface and in the bilayer interior, that is critically coupled to the lipid matrix. These modulations in solvent fluctuations are proposed to be the most sensitive in picking out weak and transient molecular interactions, long before changes in interfacial macromolecular dynamics, thermodynamics, packing, or interactions become measurable with other existing techniques.^{29,30}

The exclusive detection of local hydration dynamics by ODNP relies on the selective enhancement of ^1H NMR signals of water protons that are dipolar coupled to the electron spins of nitroxide radicals on specific site of interest. This electron-

proton dipolar coupling is critically distance-dependent (with $\sim r^{-3}$) and is only efficient when the translational correlation time of water protons is sufficiently fast with respect to the electron spin precession period of 100 ps (=1/10 GHz, inverse of electron Larmor frequency) at an operating 0.35 T magnet. Therefore, translational correlation times of hydration water on the 10–1000 ps time scale can be determined with high sensitivity, which covers all time scales of Brownian diffusive dynamics of bulk or loosely bound water.¹² Although there are other classes of hydration water (e.g., structural water) that can compose the hydration layers, especially in the first hydration layer of biomolecular surfaces, it is important to note that it is the *dynamics* of this disordered, bulk-like, water that critically couples to the dynamic changes of interactions or conformations occurring at macromolecular interfaces.²⁸ Importantly, because ODNP only excites water protons that are dipolar coupled to the localized electron spins near biomacromolecular surfaces (within 10–15 Å), ^1H NMR signals of bulk water are invisible, allowing for the selective detection of hydration water at the molecular interfaces, in the full presence of bulk water under biologically relevant conditions. Thus, ODNP is ideally suited for the sensitive and site-specific detection of hydration dynamics modulations induced by macromolecular interactions, even if the couplings are too weak to alter the structures and dynamics of the participating molecular interfaces, or to provide spectroscopic signatures of long-range, transient, intermolecular couplings in solution state that are otherwise difficult to measure.³⁰

This paper and the accompanying paper by Wang et al.¹ present two extensive studies with consistent results obtained using entirely different techniques and approaches. The major conclusion of both studies is that the biomembrane activities of the polymers can be manifested, and possibly mediated, by their

unique interactions with lipid membranes. Here, we employed ODNP analysis to explore interactions between lipid membranes and membrane-active polymers through measurements of the hydration dynamics in lipid vesicle systems, both off lipid headgroup surfaces and within the hydrophobic core of bilayers. Besides the two representative poloxamers, P188 and P181, that are widely employed clinically, we have also included the study of four additional PEO-based polymers: poloxamers P333, P335, poloxamine P1107, and PEG-8K. These candidates represent an array of polymers whose architecture and hydrophobicity are readily varied with the change of the PEO/PPO chain length and composition and, thus, serve as important control systems to adequately test the notions that biomembrane activities of these PEO-based polymers depend on their hydrophobicity and architecture. To investigate polymer–membrane interactions, effects of polymer concentration and incubation time have been systematically examined, with the latter allowing us to assess the kinetics of polymer adsorption on the surface and translocation into the lipid bilayer. Concurrent continuous-wave electron paramagnetic resonance (cw EPR) line shape analysis has also been carried out to track potential changes in local polarity or mobility of lipid headgroups and hydrocarbon tails. Our results indicate that P188 and P181, regardless of their hydrophobicity, share a common mechanism of interaction with the lipid membrane, namely surface adsorption followed by insertion into the lipid bilayer. The kinetics for this process, starting from surface adsorption to the membrane insertion of poloxamers, however, strongly depend on polymer hydrophobicity. Notably, we observed that hydrophobic P181 initially adsorbs on the membrane surface following by an insertion, whereas hydrophilic P188 only adsorbs on the membrane surface and does not insert into bilayers within our experimental time scale. While interactions of these polymers with lipid membranes are too weak to show any measurable changes in EPR line shapes, ODNP can sensitively detect the fine modulation of interfacial hydration dynamics induced by such weak interactions. Our ODNP results allow us to conclude that the poloxamer–membrane interaction is of subtle and weak nature, and the interfacial hydration dynamics, just as proposed, is exquisitely sensitive for unraveling molecular details of interactions between prominent polymers and lipid membranes.

2. THEORETICAL BASIS

ODNP relies on the polarization transfer from unpaired electrons of nitroxide radicals to water protons through dipolar and/or scalar coupling. It gives rise to selectively enhanced ^1H NMR signals of hydration water close to ($\sim 10 \text{ \AA}$) the localized spin labels upon saturating the electron spin resonance transition by strong cw microwave irradiation. The negative ^1H NMR signal enhancement of hydration water can be observed only if the time scale of translational motion of hydration water is rapid enough to induce electron–proton flip–flip dipolar cross relaxation.³¹ The ODNP technique requires the acquisition of the enhanced ^1H NMR signals at various microwave powers. The maximal enhancement value E_{\max} driven by ODNP, can be obtained by extrapolating the microwave power to an infinite value^{11,12,31}

$$E_{\max} = 1 - \xi f_{\max} \frac{|\gamma_e|}{\gamma_N} \quad (1)$$

where ξ is the coupling factor that describes the electron–proton interactions and contains key information about hydration dynamics, f is the leakage factor describing how efficiently the electron spin relaxes the proton spin relative to other relaxation sources, s_{\max} is the maximum electron spin saturation factor, and γ_e and γ_N are the gyromagnetic ratios of the electron and proton spins, respectively, providing $|\gamma_e|/\gamma_N = 658$. In order to assume $s_{\max} = 1$, full saturation of all EPR transitions and, thus, complete exchange of hyperfine lines of nitroxide radical needs to be achieved, given that microwave frequency irradiation at a single frequency in cw mode is employed. Indeed, for nitroxide radicals tethered to slow tumbling macromolecules, such as proteins or lipid vesicles, the condition of $s_{\max} \approx 1$ is met, even at dilute spin label concentrations (i.e., 1–2 mol %).^{11,12,32} Fundamentally, the ODNP-induced ^1H NMR signal enhancement depends on the spin label concentration. For example, at a higher spin-label concentration, the protons have increased chances to collide with nitroxide spin labels and, thus, to achieve higher ^1H spin polarization during the nuclear T_1 time scale. This effect is, however, accounted for with the leakage factor, f , that can be quantified by measuring the longitudinal relaxation times of samples in the presence (T_1) and absence (T_{10}) of the spin labels, following $f = 1 - T_1/T_{10}$.^{11,12} The electron–proton coupling factor, ξ , can then be quantitatively determined, because all the other parameters in eq 1 are now known. Most importantly, ξ does not depend on spin-label concentration, but carries information of the translational dynamics of ^1H -bearing molecules in solution with respect to spin labels. When the nitroxide free radical is fully hydrated, the coupling between water proton and electron spin of radical is dominated by dipolar interaction, and the fluctuation of electron–proton dipolar interaction due to translational diffusion dynamics can be expressed by a single translational correlation time, τ . Thus, a single spectral density function $J(\omega, \tau)$ can describe the interaction. The coupling factor for dipolar interaction between electron and proton spins, assuming translational diffusion between two spins is the dominant mechanism to cause cross relaxation, is given by³¹

$$\xi = \frac{6J(\omega_e + \omega_N, \tau) - J(\omega_e - \omega_N, \tau)}{6J(\omega_e + \omega_N, \tau) + 3J(\omega_N, \tau) + J(\omega_e - \omega_N, \tau)} \quad (2)$$

where ω_e is the electron spin Larmor frequency, ω_N is the nuclear spin Larmor frequency, and τ is the translational correlation time between the electron and the ^1H nuclear spin. In this study, we performed all ODNP experiments at a 0.35 T magnet, where $\omega_e \sim 10 \text{ GHz}$ and $\omega_N \sim 15 \text{ MHz}$. According to eq 2, the coupling factor ξ specifically dominates by the much higher electron spin Larmor frequency, ω_e . In this regime, the closer τ is to 100 ps ($=1/10 \text{ GHz}$), the more sensitively the variation in water mobility modulates ξ . Typically, τ on the order of several tens or hundreds of picoseconds is caused by the free or retarded translational diffusive motion of disordered, bulk-like, water in solutions. Once the coupling factor is obtained by the measurement of E_{\max} and f , the translational correlation time τ of hydration water with the interacting species can be extracted using the appropriate spectral density function $J(\omega, \tau)$. We employed the force-free hard-sphere dynamic model (in eq 2) that has been shown to adequately describe the surface relaxation in spin-labeled soft matter systems, whose hydration dynamics is mediated by translational diffusion.³³ This model has been demonstrated to provide

reliable and consistent fit parameters in several systems.^{12,15,17,32,34–37} The detailed analysis of τ and ξ are presented elsewhere.^{11–13} Here, the τ value extracted from ODNP experiments is inversely proportional to the translational diffusion coefficient of the local hydration water, D , following $\tau = d^2/D$, where d is the distance of closest approach between the electron spin and the proton of water.^{12,31} We have recently determined that the translational correlation time of bulk water, τ_{bulk} , is 32.9 ps by ODNP method (i.e., $\xi = 0.33$) at 0.35 T.¹³ This value is in good agreement with the literature value deduced by a combination of ODNP and pulsed ESR techniques,³⁸ field cycling relaxometry measurements, and computational studies.^{39,40} A value of $\tau_{\text{bulk}} = 32.9$ ps also means that the electron–¹H distance of closest approach that modulates the ODNP effect is $d = 3$ Å. Therefore, the most important quantity of interest is D and τ values for the hydration water, as well as the dynamic retardation factor,²⁶ which is known as the average translational correlation time of the hydration water within the distance of closest approach of nitroxide spin label divided by the translational correlation time of bulk water, $\langle \tau \rangle / \tau_{\text{bulk}}$.

In summary, ODNP allows us to quantify the diffusivity of hydration water close to the localized spin labels on macromolecular assembly or soft matter systems, by measuring E_{max} and f at 0.35 T. Important strengths of the ¹H ODNP method include high sensitivity, requiring only minute sample quantities and dilute concentrations (typically ~4 μL and ~100 μM spin-label concentrations), time-resolved probing with ~1 s resolution, concurrent X-band cw EPR line shape analysis to obtain local molecular dynamics, and the capability to probe hydration dynamics in deeply buried as well as solvent-exposed molecular interfaces. Furthermore, this newly developed technique has been employed, thus far, for probing translational hydration dynamics in the lipid vesicle systems,^{32,34,41} interfaces of polyelectrolytes involved in complex coacervation,³⁷ as well as biomolecular interfaces involved in protein folding of apomyoglobin¹⁵ and early tau protein oligomers and aggregates.¹⁷

3. EXPERIMENTAL METHODS

Materials. Phospholipids 1,2-dioleoyl-sn-glycero-3-phosphocholine (DOPC) and a headgroup spin-label, 1,2-dioleoyl-sn-glycero-3-phospho(tempo)choline (PC-TEMPO), were purchased from Avanti Polar Lipids Inc. (Alabaster, AL). A lipid tail spin-label, 16-doxyloctanoic acid (16-DSA), contained a nitroxide spin label at the 16th carbon position was purchased from Sigma Aldrich (St. Louis, MO). All poloxamer samples were generous gifts of BASF (Wyandotte, MI). Poloxamine P1107 and PEG-8K were purchased from Sigma Aldrich. The physical properties of all the polymers used in this study were listed in Table 1. All the samples were used as received.

Table 1. List of Polymers and Their Physical Properties at Room Temperature

polymer	MW (g/mol)	<i>m</i>	<i>n</i>	HLB ^a	CMC ^b (μM)
P188	8400	27	80	29	125
PEG-8K	8000	0	182	hydrophilic	
P1107	15000	20	58	24	(no data)
P335	6500	56	37	15	(no data)
P333	4950	60	17	9	30
P181	1750	32	2	3	<50

^aHLB: hydrophilic–lipophilic balance. ^bCMC: critical micelle concentration.

Preparation of Phospholipid Vesicles. Large unilamellar vesicles (LUV) were prepared according to the conventional thin-film hydration method.⁴² Briefly, a stock DOPC lipid was prepared in a chloroform/methanol (9:1, v/v) mixture. The desired amount of stock lipid was transferred into a glass vial. The solvent was then dried under a faint N₂ gas stream, and the thin film was thoroughly dried in a desiccator connected to a mechanical vacuum pump. The dry lipid films were hydrated with Millipore water at 37 °C for 1 h, followed by vortexing for 1 h. The dispersions were subsequently extruded 21 times through a polycarbonate membrane with 200 nm diameter pore size at room temperature. The same batch of vesicle sample was used for each set of experiments. Fresh vesicle samples were used for all the measurements. The final lipid concentration is 32 mM. The concentration of spin label is 675 μM. The DOPC lipid membrane is in fluid phase at room temperature. Polymer-vesicle samples were prepared in two different methods: (1) an aliquot of polymer was mixed with lipid vesicles to reach a desired concentration. EPR and DNP measurements were then started within approximately 5 min upon mixing the polymer with vesicles; (2) the polymer was codried with lipids at the desired concentration, and then the vesicle sample, with polymer preincorporated, was prepared.

ODNP and EPR Experiments. ¹H ODNP experiments were performed at a 0.35 T electromagnet, operating at 14.8 MHz ¹H Larmor frequency and at 9.8 GHz electron Larmor frequency. A 3.5 μL sample was loaded in a 0.6 mm I.D. quartz capillary tube (Fiber Optic Center Inc., New Bedford, MA) and sealed at both ends with beeswax. The capillary was mounted on a home-built NMR probe with a U-shaped NMR coil. EPR spectra were acquired on a Bruker (Billerica, MA) X-band EMX EPR spectrometer with a rectangular TE₁₀₂ cavity at 20 mw incident microwave power, by using a field modulation of 1.5 G. During ODNP experiments, the center field of nitroxide hyperfine transition lines was pumping continuously by microwave irradiation at 9.8 GHz, while ¹H NMR signal was recorded. To avoid sample heating during microwave irradiations, dry air was blown through the sample at a steady rate to keep the temperature constant. T_1 relaxation measurements were carried out by an inversion–recovery pulse sequence operated by either Kea (Magritek Limited, Wellington, New Zealand) or Bruker Avance spectrometer in a 0.35 T superconductive magnet. A standard 90° pulse length was about 4 μs. The typical experimental time for T_1 experiment was about 20 min and for ODNP experiment was about 10 min. All the experiments were performed at room temperature.

4. RESULTS AND DISCUSSION

Probing Interfacial Hydration Dynamics of Lipid Membranes. ODNP was employed to measure the translational correlation time τ of hydration water dipolar coupled to the electron spin probes off the headgroup of a phospholipid, PC-TEMPO, and on the lipid tail of a surfactant, 16-doxyloctanoic acid (16-DSA).^{30,32,34,35} Both of these probes have been demonstrated to be viable for the study of lipid dynamics and polarity in various lipid membrane systems by cw EPR^{43,44} and paramagnetic relaxation enhancement NMR measurements.⁴⁵ To minimize perturbation to the lipid bilayer, a low concentration of the spin-label probes (~1 mol %) that has been verified to not affect lipid packing by means of leakage experiments³⁴ was used in this study. Overall, the nitroxide spin label of PC-TEMPO locates *above* the choline moiety and extends into the aqueous phase, spanning 3–4 water layers (~10 Å) off the membrane surface.⁴⁶ The EPR spectral line shapes suggest that this spin label presents sufficient motional freedom to probe the lipid headgroup volume.^{30,32} The nitroxide spin label of 16-DSA locates *within* the lipid bilayer core and shows even considerably greater motional freedom than that of PC-TEMPO and, thus, enables to probe a larger, yet local, volume within the bilayer core.^{30,34,43}

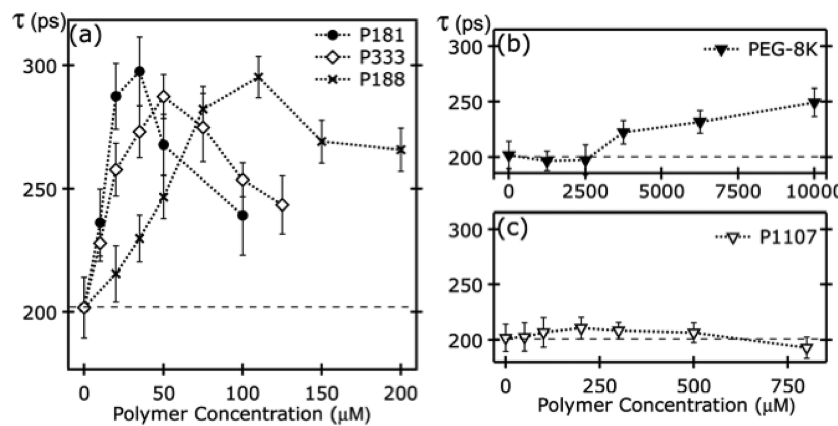


Figure 1. Translational correlation time of surface hydration dynamics (as probed by PC-TEMPO) of DOPC lipid vesicles upon introducing (a) P181 (HLB = 3), P333 (HLB = 9), and P188 (HLB = 29), (b) PEG-8K, and (c) poloxamine P1107, at 0 incubation time, as a function of polymer concentration. Error bar represents the standard deviation.

In polymer-free DOPC vesicles, the translational correlation time, τ , of surface water is ~ 200 ps, which is about 6-fold impeded compared to that of bulk water.⁴⁷ τ of the minute quantity of intrabilayer water is ~ 400 ps, which is another 2-fold slower compared to that of the lipid membrane surface water. Even though this impeded intrabilayer water diffusion is expected, it is still faster than the water dynamics found in the compact and dry hydrophobic core of a folded protein (typically $\tau > 900$ ps).¹⁵ Our recent work has demonstrated that such fast water diffusion in the bilayer core can be reconciled with a transient water pore model.³⁴ In this context, it is important to note that fast water dynamics do not imply high water content at all. In fact, the lipid bilayer interior is nearly “dry”,⁴⁸ yet the few water molecules (less than one water molecule per lipid) percolate through the lipid bilayer quite efficiently and fast,³⁴ as they can be derived from the known, fast, basal water permeability across a lipid bilayer.⁴⁹

Regarding the interactions between these polymers and the lipid membrane, we anticipate the surface hydration dynamics to be affected by collisions between the polymer and the lipid surface within ~ 10 Å of the surface probes. On the other hand, the interior hydration dynamics can be altered either by direct collisions between the polymer and the intrabilayer volume (i.e., polymer insertion) or by the indirect effect of slowed membrane interfacial solvent fluctuations. More specifically, we hypothesize that the “membrane sealing” effect of the hydrophilic poloxamer arises from its ability to either physically tighten the lipid membrane (i.e., changes in lipid packing) or suppress membrane interfacial fluctuations (i.e., changes in local hydration and lipid dynamics at the lipid headgroup region, but no changes in the overall lipid packing). To rule out one versus the other, EPR line shape analysis was used to provide a reference, as changes in overall lipid packing and dynamics would reflect itself clearly in changes in the EPR line shape, almost regardless of the position of the spin label, while changes in the local lipid fluctuations or hydration dynamics might not be observable by changes in the EPR line shape, depending on the exact probe location and time scale for the dynamics involved. With this set of knowledge and assumptions in mind, we have analyzed the modulation of hydration dynamics, both at the lipid membrane surface and in the bilayer interior, upon addition of polymers to DOPC lipid vesicle solutions at a varying range of polymer concentration and incubation time.

Interactions between Polymers and Lipid Vesicles: Observed through Hydration Dynamics. *a. Changes in Surface Hydration Dynamics as Polymers Interact with the Membrane Surface.* We examined six PEO-based polymers with different architecture and hydrophobicity, as listed in Table 1. They can be generally grouped into hydrophilic polymers (i.e., P188, PEG-8K, and P1107) and hydrophobic polymers (i.e., P181, P333, and P335). Figure 1 depicts ODNP analysis on surface spin-labeled DOPC vesicles right after the addition of polymers at various polymer concentrations. Given that polymer–membrane interactions evolve over several hours, we label these measurements as “0 incubation time”. The dashed line in Figure 1 denotes τ value for polymer-free DOPC vesicles, which serves as the baseline for comparison with τ obtained in the presence of the polymers. It is important to note that at 0 incubation time all types of polymers employed in this work either only adsorbed on the membrane surface or interacted with the extended volume of lipid headgroups and did not have the opportunity to fully insert into the bilayer interior.

As shown in Figure 1a, the hydration dynamics on the membrane surface upon polymer adsorption exhibit a distinct trend with poloxamer concentration. At concentrations below the critical micelle concentration (CMC) of each poloxamer, the τ value increases gradually (i.e., water diffusivity is slowed) with increasing poloxamer concentration and eventually reaches its maximum value close to the CMC. Above the CMC, τ value establishes a plateau that is less than its maximum. It is quite interesting that all three poloxamers, even though at different polymer concentrations, retard the surface water diffusivity to a similar degree, evidenced by their comparable ceiling τ of ~ 300 ps despite their distinct CMCs. This finding suggests the existence of an “optimal” state to which the poloxamers can drive the surface hydration dynamics. Among these poloxamers, the most hydrophobic poloxamer P181 requires the least amount to retard surface hydration dynamics to the maximum level, thus, implying that P181 has the strongest effect on the hydration dynamics close to the membrane surface at 0 incubation time.

To investigate what role the PPO and PEO blocks play in the polymer–membrane interactions, we studied the interactions between lipid membranes and the homopolymer PEG-8K. This homopolymer has a molecular weight similar to P188, but only consists of PEO blocks and does not have the hydrophobic

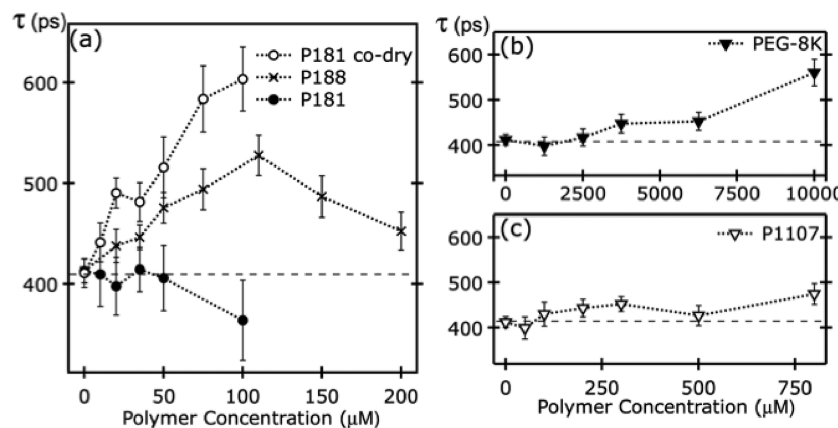


Figure 2. Translational correlation time of intrabilayer hydration dynamics (as probed by 16-DS) of DOPC lipid vesicles upon introducing (a) P181 (HLB = 3), P188 (HLB = 29), (b) PEG-8K, and (c) poloxamine P1107 at 0 incubation time as a function of polymer concentration. The open circles in (a) represent the vesicles preincorporated with P181. In this case, P181 incorporates into the bilayer interior.

PPO block. Therefore, it was used as a control to illustrate the role of PPO blocks. As shown in Figure 1b, PEG-8K can impede the dynamics of surface water, but its effect becomes noticeable only at concentrations above 2.5 mM, which is more than \sim 100 times higher than the concentration of P188 used. Above that concentration, the degree of retardation in hydration dynamics grows proportionately with polymer concentration, as anticipated. This is reasonable as PE-8K does not assemble or aggregate in solution and, thus, has no CMC. Without such limitation of aggregation formation, the accumulation of PEG-8K polymer chains around the lipid vesicle surface simply increases with increasing polymer concentrations. It should be emphasized that even though the viscosity of bulk water increases at high PEG-8K concentrations, this does not affect our ODNP measurements; the strength of the ODNP approach is to measure *local* hydration dynamics on lipid membrane surfaces impeded by adsorbed PEG-8K, rather than by the bulk viscosity effects caused by the polymers. For example, we found that the increased viscosity in a 10 mM PEG-8K solution would reduce bulk water diffusivity by \sim 25%. However, upon addition of the same concentration of PEG-8K to the DOPC vesicle solution, the local hydration dynamics measured at the membrane surface retards by \sim 40%, suggesting that PEG-8K has a greater effect on the local surface water diffusivity than the bulk water diffusivity. Still, in comparison to the effect of P188 at the same polymer concentration, the impact of PEG-8K on lipid membrane surface hydration is much lower. This suggests that PEG-8K interacts rather weakly with the lipid bilayer, in good agreement with previous observations that PEG requires much higher concentrations than P188 to exert its biomedical functions (e.g., in promoting cell fusion or membrane sealing^{50,51}). Consequently, we suggest that the hydrophobic PPO block in P188, that differentiates P188 from PEG-8K, plays an essential role in driving P188 to effectively interact with the lipid membrane surface.

Given that the polymer architecture could also affect its biomembrane activities, we used poloxamine P1107 as a control polymer to study the effect of the polymer shape. Poloxamine P1107 is a four-armed PPO-*b*-PEO block copolymer connected by a diamine core. This configuration renders P1107 a much bulkier structure than the linear poloxamer, and hence, we anticipate that it may affect surface hydration dynamics of lipid membranes more drastically than poloxamers. Contrary to our

expectation, we found that P1107 barely interacts with the lipid membrane surface, evidenced by the fact that its presence only leads to minute variations in the surface hydration dynamics of lipid membranes (Figure 1c), even at very high concentrations ($>500 \mu\text{M}$). Moreover, the τ values of surface water remain almost unaltered upon addition of 200 μM of P1107 to both zwitterionic DOPC vesicles ($\tau = 211 \pm 13 \text{ ps}$) and negatively charged vesicles composed of 90% DOPC and 10% DOPG ($\tau = 186 \pm 15 \text{ ps}$). As P1107 has the same subunits as P181 and P188, the lack of interactions between P1107 and lipid membrane (Figure 1c) is not due to the charge mismatch between the polymer and the lipid membranes surface, but rather the bulky architecture of the PEO polymer chains, as they likely hinder the small, but critical, PPO midblock to approach the lipid membrane surface. In light of this observation, we conclude that the architecture of the polymer also plays an important role in modulating interactions of polymers with lipid membranes.

b. Changes in Interior Hydration Dynamics as Polymers Interact with the Membrane Surface. Figure 2 represents ODNP analysis of DOPC vesicles with spin labels within the bilayer core right after the addition of polymers at various polymer concentrations. It should be noted that under the experimental conditions, at 0 incubation time, we confirmed that there is no direct collision between the polymers and the intrabilayer volume (i.e., polymer insertion). Still, we observed that all hydrophilic polymers (P188, PEG-8K, and P1107) caused significant retardation in the hydration dynamics within lipid bilayers, and the retardation trend over the polymer concentrations is fairly similar to that found on the membrane surfaces. One rational interpretation of these observations is that the large hydrophilic PEO blocks of these polymers can weakly dampen the fluctuations of *surface* hydration and lipid dynamics, which in turn induces the modulation of *intrabilayer* hydration dynamics. It should be noted that this type of interaction is subtle but very distinct and has been previously observed when salts (e.g., sodium chloride) or small amphiphilic molecules (e.g., ethanol) were added to lipid vesicles.³⁴ Without measurably altering lipid dynamics on the membrane surface or in the interior, both types of molecules can significantly slow intrabilayer water diffusion.^{34,49}

The hydrophobic poloxamer P181, on the contrary, shows the entirely opposite effect on intrabilayer hydration dynamics. As illustrated in Figure 2a (closed circles), the intrabilayer

hydration dynamics does not exhibit any noticeable change upon the addition of P181 up to a concentration of 50 μM ; however, once the P181 concentration is increased to 100 μM , an ~10% increase in water diffusivity is observed. Such an increase is likely due to the initial insertion of the poloxamer below the headgroup region that serves to pry and open the packing of acyl chains at the headgroup/tail interface. This effect explains why P188 increases the permeation of molecules across the biomembrane.^{5,6} To further test this hypothesis, we preincorporated P181 into lipid membranes by codrying the polymer with the lipids and then rehydrating them together. In this case, the hydrophobic PPO block of P181 is known to be fully incorporated with the hydrophobic lipid tails and thus represents the situation of a complete interaction of P181 with the lipid interior volume. The open circles in Figure 2a display the interior hydration dynamics of the lipid vesicles with P181 preincorporated into the lipid membrane at various concentrations. Interestingly, intrabilayer water diffusion of these samples becomes rather retarded, and the retardation linearly increases with the P181 concentration. This observation indicates that as the PPO block fully incorporates into the lipid bilayer, it can directly collide with the interaction volume of bilayer interior, thus, efficiently tightening and retarding the intrabilayer hydration dynamics. It can also support our hypothesis in that the significant increase in intrabilayer hydration dynamics at high P181 concentration does not arise from full insertion of P181 into a bilayer interior, but from the embedding of P181 underneath the headgroup region, in close proximity to the headgroup/tail interface.

c. Changes in Interior Hydration Dynamics as Polymers Gradually Insert into the Bilayer over Time. To further elucidate the transition process from initial adsorption to full insertion, we studied the kinetics of P181 insertion into lipid membranes. Figure 3 represents the τ value of intrabilayer

observed at 0 incubation time at low P181 concentrations is likely due to a low collision rate between P181 and the interaction volume of lipid bilayers. In contrast, this characteristic entirely turns around at incubation time longer than 3 h, at which time the intrabilayer hydration dynamics is gradually retarded over time until a plateau is reached at ~5 h. Because the full insertion of the PPO group of preincorporated P181 can efficiently impede intrabilayer water diffusivity (see Figure 2a), the onset of decrease in intrabilayer water diffusivity indicates the beginning of the transition from initial insertion of the PPO segment of P181 to its full insertion into the bilayer interior. Similar characteristics are also observed with the other two hydrophobic poloxamers, P333 (Figure 3, closed diamonds) and P335 (Figure 3, open triangles). In all the cases, the more hydrophilic the poloxamer is, the slower the onset of the transition and plateau of maximum τ value reach. For example, it takes ~5 h for P333 to elicit the onset and ~8 h to reach its plateau; it takes ~7 h for P335 to elicit its onset and ~11 h to reach its plateau. Because polymer hydrophobicity decreases from P181 to P333 to P335, the delayed onset of the transition among these three polymers suggests that the insertion kinetics of poloxamer into lipid membranes is critically modulated by the polymer hydrophobicity. This finding is in excellent agreement with the two-state transition mechanism proposed by Wang et al. in that poloxamers initially accumulate themselves at the membrane surface, prior to the complete insertion into the lipid bilayer with time.⁵² It also illustrates that polymer hydrophobicity is indeed the driving force to facilitate polymer insertion into the lipid bilayer, as reported in the accompanying paper.¹

Contrarily, intrabilayer water diffusivity in the presence of the hydrophilic poloxamer P188 exhibits a different time-dependent behavior, as shown in the inset of Figure 3. Over the time scale of our measurements (~45 h), P188 overall slows intrabilayer hydration dynamics, with slightly increasing at ~45 h. It implies that P188 only adsorbs on the membrane surface at ~45 h incubation. Given that the hydrophilic P188 is highly unfavorable to insert into the hydrophobic core of bilayer, it is likely that the full insertion of P188 into bilayer interior would occur if a sufficient long incubation period is given (e.g., several days).⁵² Thus, we conclude that all the poloxamers, regardless of their hydrophobicity, can initially adsorb on the membrane surface and then gradually insert into bilayer cores. This insertion kinetics strongly depends on the hydrophobicity of poloxamer.

To further scrutinize the characteristics of the two-state transition process,⁵² we compare the surface and interior hydration dynamics as a function of P181 concentration at 0 h incubation time (P181 only interacts with membrane surface) and at 7 h incubation time (P181 has inserted into bilayer interior), as summarized in Figure 4. It has been discussed earlier that, at 0 h incubation time, P181 can adsorb on the membrane surface and embed below headgroup region at higher P181 concentration. At 7 h incubation of P181, at which time the PPO block of P181 inserts into bilayer interior, the τ values of surface water exhibit to be independent of polymer concentration (open squares, Figure 4a), whereas the τ values of intrabilayer water clearly changes with increasing P181 concentration (open squares, Figure 4b), with a trend that is very similar to τ of surface water at 0 incubation time with P181 (closed circles, Figure 4a). Thus, this observation conforms the two-state transition mechanism⁵² in that P181 can initially adsorb on the membrane surface; after longer incubation time,

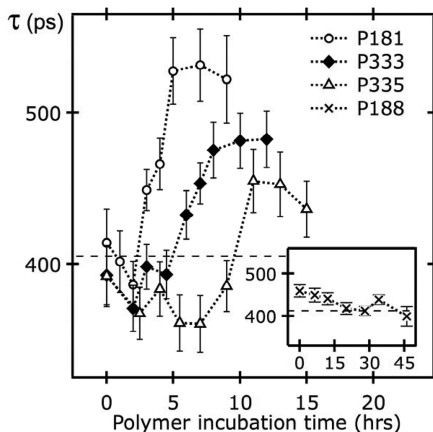


Figure 3. Translational correlation time of intrabilayer hydration dynamics of DOPC vesicles in the presence of 30 μM of P181 (open circles), P333 (closed diamonds), P335 (open triangles), and P188 (the inset) as a function of incubation time.

water in the presence of 30 μM P181 over time. In addition, the same measurements were performed using P333, P335, and P188 to explore the effect of polymer hydrophobicity on its insertion into bilayers. As the lipid vesicles incubated with P181 up to 3 h, their intrabilayer water dynamics increase by ~7%, consistent with the case of the high P181 concentration at 0 incubation time (see Figure 2a). It implies that the absence of measurable changes in intrabilayer hydration dynamics

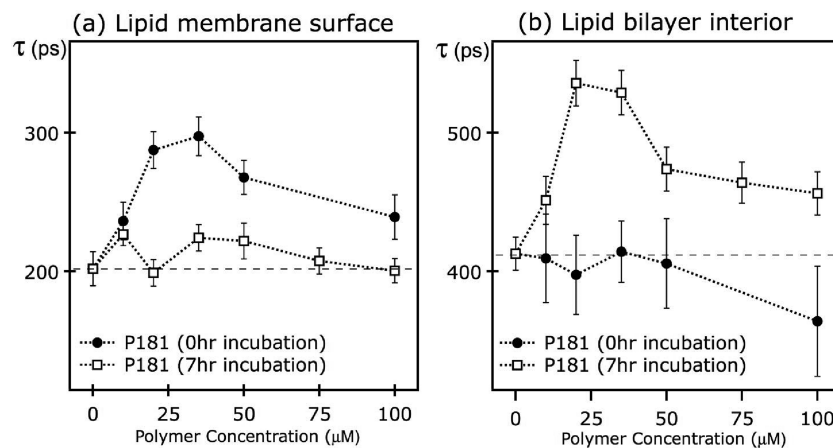


Figure 4. Translational correlation time of (a) surface hydration dynamics and (b) intrabilayer hydration dynamics of DOPC vesicles in the presence of P181 at 0 incubation time and after 7 h of incubation. Error bar represents the standard deviation.

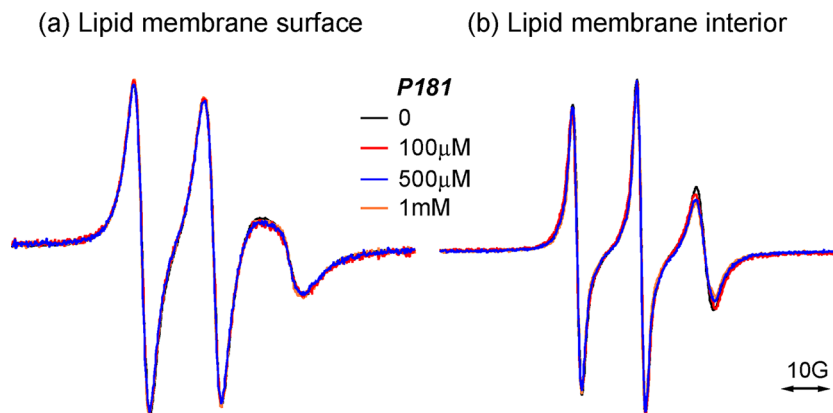


Figure 5. X-band cw EPR spectra of the polymer-free DOPC vesicles and vesicles preincorporated with P181 with spin labels (a) on the vesicle surface and (b) in the interior of the lipid bilayer as a function of polymer concentration.

it may be completely buried below the headgroup region or in the lipid bilayer, with very little P181 left outside the vesicles.

Interactions between Polymers and Lipid Vesicles Observed through Lipid Dynamics. Figure 5 exhibits the representative EPR spectra of the polymer-free DOPC vesicles and the vesicles with preincorporated P181 with spin labels both at the headgroup (PC-TEMPO) and in the bilayer interior (16-DSA). For the headgroup-labeled polymer-free vesicles, its EPR spectrum shows the significantly broadened line shape compared to that of the bilayer interior-labeled vesicles. This is because the rotational motion of PC-TEMPO probes is restricted by the strong electrostatic interactions with other neighboring headgroups. In contrast, 16-DSA probes show a higher degree of rotational freedom, as they are attached to the fairly flexible acyl chains of phospholipid tails. Nevertheless, we found that no measurable changes of EPR line shapes were detected under our experimental conditions, regardless of polymer concentration and spin-label position, even in the vesicle systems that are ensured to have the polymer physically incorporated into bilayer interior. In fact, this remains true for all polymers investigated in this study. It is known that the EPR line shape is very sensitive to changes in the overall lipid packing and dynamics.⁸ Therefore, the unaltered EPR line shape in lipid systems generally represents an absence of changes in the lipid dynamics or packing. Because a series of our ODNP data have clearly explored the interactions of the polymer with the lipid bilayer, the unaltered EPR line shape in

this study implies that the polymer–lipid interactions is too weak to cause measurable changes in lipid dynamics.³⁰ Therefore, this finding showcases that ODNP is indeed a highly sensitive method for probing weak molecular interactions through the fine modulation of interfacial hydration dynamics with site-specificity under physiological conditions.

Mechanism of Molecular Interactions of Lipid Membranes with P181 and P188. In light of our ODNP and EPR results, we propose the molecular mechanism of interactions between lipid membranes and two representative poloxamers, P181 and P188, as illustrated in Figure 6. We revealed that both poloxamers share a common mechanism of interaction with the lipid membrane, with a surface adsorption followed by an insertion; however, the kinetics for these processes are very different. For P181, the more hydrophobic PPO block favors to interact with the lipid tails rather than the lipid headgroups; on the other hand, the hydrophilic PEO chains are too short to effectively hold the entire polymer chain on the membrane surface. As a result, P181 can quickly embed itself below lipid headgroups right after initial interaction with lipid membranes (Figure 6a). When more time is given to P181, it eventually inserts into the bilayer interior (Figure 6b). On the other hand, when P188 is shortly added in the vesicle solution, its hydrophobic PPO block facilitates the polymer to approach the membrane surface, while its large hydrophilic PEO blocks could form hydrogen-bonding networks with the surface hydration layers of the lipid membrane headgroups

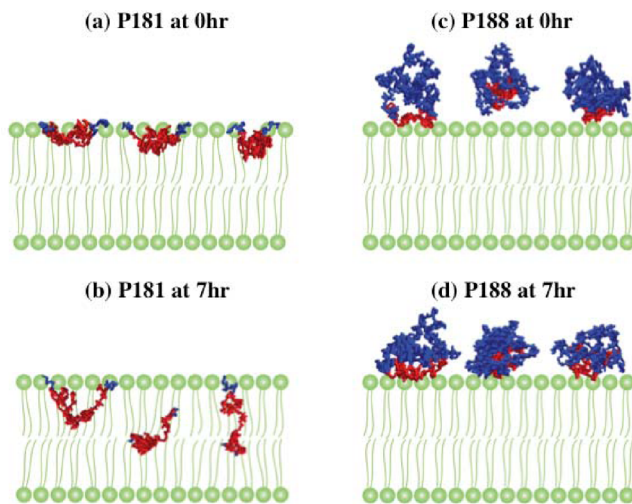


Figure 6. Schematic interactions of lipid membranes with P181 and P188 at 0 incubation time and after 7 h incubation.

(Figure 6c). This configuration in turn makes it capable of dampening interfacial solvent fluctuations at lipid membrane surfaces, evidenced by the reduction of water diffusivity, both on the surface and in the bilayer interior of the lipid membrane. Because the PPO block thermodynamically favors the interaction with hydrophobic lipid tails, it could eventually drive the polymer, becoming much closer to the lipid headgroups at the relatively long incubation period (Figure 6d).

5. DISCUSSION

It has been demonstrated in the accompanying paper that the presence of the hydrophilic polymers (i.e., P188, PEG-8K, and P1107) can efficiently protect lipid vesicles from lipid peroxidation, whereas the presence of the hydrophobic poloxamers fails to do so.¹ This finding unambiguously supports our hypothesis that the biomembrane activities of these PEO-based hydrophilic polymers are primarily due to their initial interactions with lipid membranes. Early *in vitro* studies suggested that the membrane sealing effect of P188 arises from its ability to fill the defects of lipid membranes and consequently tighten lipid packing.^{2–4,52} In this work, we revealed that P188 could exert its unique membrane sealing function through effectively dampening the fluctuation of surface and intrabilayer hydration dynamics upon interaction but not transposing in the bilayer interior nor affecting the overall lipid packing or dynamics.

On the other hand, it has been discovered that P181 can enhance the uptake of antitumor drugs in a variety of drug resistance tumor cells.⁶ Previous studies have also demonstrated that the PPO block in poloxamers is essential in the translocation of the poloxamer through lipid membranes.^{52,53} ODNP results clearly revealed that the hydrophobic PPO block of P181 initially embeds below the headgroup region and opens the packing of acyl chains at headgroup/tail interfaces. This effect strongly associates with P181 functions for accelerating the passage of molecules across cell membrane.

Most importantly, despite their different hydrophobicity, P188 and P181 share a common two-state mechanism of interaction with the lipid membrane: surface adsorption followed by insertion into the lipid membrane. Finally, ODNP can sensitively detect the weak, yet essential, poloxamer–membrane interactions through the fine modu-

lation of hydration dynamics under physiological conditions, which is difficult to study by any other existing tools. This exquisite analytical tool with unique sensitivity and site-specificity can be employed to unveil the underlying mechanisms of weak macromolecule–membrane interactions.

6. CONCLUSIONS

The interactions of lipid membranes with a series of PEO-based membrane active polymers were probed via local membrane hydration dynamics measured by a recently developed ODNP technique. We found that the hydrophilic poloxamer P188 only absorbs on the surface of lipid membranes, yet could exert its membrane sealing function by dampening membrane fluctuations, evidenced by its ability to retard surface and intrabilayer water diffusivity. Contrarily, the hydrophobic poloxamer P181 slightly loosens the lipid packing during initial embedding below the lipid headgroups, thereby acting as a membrane permeabilizer. Our study demonstrates that the polymer interactions with lipid membranes as well as their corresponding biomembrane functions can be affected by several factors, including the size, architecture, and hydrophobicity of the polymer, the polymer-to-lipid ratio, and the incubation time. Among these factors, we conclude that polymer hydrophobicity and architecture play a key role in dictating these interactions and functions. Finally, ODNP can provide superior sensitivity and site-specificity to probing the modulation of interfacial hydration dynamics upon macromolecular interactions. It can be a unique and generally applicable technique for exploring interactions of lipid membranes with other biomolecules, such as proteins and peptides, under physiological conditions, whose mechanisms are essential to gain insight into biological functions.

■ AUTHOR INFORMATION

Corresponding Author

*E-mail: kayelee@uchicago.edu; songi@chem.ucsb.edu.

Author Contributions

[†]These authors contributed equally.

Notes

The authors declare no competing financial interest.

■ ACKNOWLEDGMENTS

C.-Y.C., R.K., and S.H. acknowledge support by the UCSB NSF-MRSEC Program (DMR-0520415 and DMR-1121053), the NSF Faculty Early CAREER Award (CHE-0645536), and the Packard Fellowship for Science and Engineering. C.-Y.C., R.K., and S.H. made use of shared experimental facilities of the Materials Research Laboratory: an NSF MRSEC, supported by NSF DMR 1121053. The MRL is a member of the NSF-supported Materials Research Facilities Network (www.mrfn.org). J.-Y.W. and K.Y.C.L. are grateful for the support of the March of Dimes (No. 6-FY07-357), the NSF (MCB-0920316), and the University of Chicago NSF-MRSEC program (DMR-0820054).

■ REFERENCES

- Wang, J.-Y. M.; Marks, J. M.; Lee, K. Y. C. 10.1021/bm300847x.
- Mina, E. W.; Lasagna-Reeves, C.; Glabe, C. G.; Kayed, R. *J. Mol. Biol.* **2009**, 391 (3), 577–585.
- Yasuda, S.; Townsend, D.; Michele, D. E.; Favre, E. G.; Day, S. M.; Metzger, J. M. *Nature* **2005**, 436 (7053), 1025–1029.

- (4) Greenebaum, B.; Blossfield, K.; Hannig, J.; Carrillo, C. S.; Beckett, M. A.; Weichselbaum, R. R.; Lee, R. C. *Burns* **2004**, *30* (6), 539–547.
- (5) Krylova, O. O.; Melik-Nubarov, N. S.; Badun, G. A.; Ksenofontov, A. L.; Menger, F. M.; Yaroslavov, A. A. *Chem.—Eur. J.* **2003**, *9* (16), 3930–3936.
- (6) Venne, A.; Li, S. M.; Mandeville, R.; Kabanov, A.; Alakhov, V. *Cancer Res.* **1996**, *56* (16), 3626–3629.
- (7) Beschiaschvili, G.; Seelig, J. *Biochemistry* **1990**, *29* (1), 52–58.
- (8) Hubbell, W. L.; Gross, A.; Langen, R.; Lietzow, M. A. *Curr. Opin. Struct. Biol.* **1998**, *8* (5), 649–656.
- (9) Celia, H.; Wilson-Kubalek, E.; Milligan, R. A.; Teyton, L. *Proc. Natl. Acad. Sci. U.S.A.* **1999**, *96* (10), 5634–5639.
- (10) Seelig, J. *Biochim. Biophys. Acta, Biomembr.* **2004**, *1666* (1–2), 40–50.
- (11) Armstrong, B. D.; Han, S. *J. Chem. Phys.* **2007**, *127* (10), 10.
- (12) Armstrong, B. D.; Han, S. *J. Am. Chem. Soc.* **2009**, *131* (13), 4641–4647.
- (13) Franck, J.; Han, S. arXiv:1206.0510v1.
- (14) Marrink, S. J.; Berkowitz, M.; Berendsen, H. J. C. *Langmuir* **1993**, *9* (11), 3122–3131.
- (15) Armstrong, B. D.; Choi, J.; Lopez, C.; Wesener, D. A.; Hubbell, W.; Cavagnero, S.; Han, S. *J. Am. Chem. Soc.* **2011**, *133* (15), 5987–5995.
- (16) Ebbinghaus, S.; Kim, S. J.; Heyden, M.; Yu, X.; Heugen, U.; Gruebele, M.; Leitner, D. M.; Havenith, M. *Proc. Natl. Acad. Sci. U.S.A.* **2007**, *104* (52), 20749–20752.
- (17) Pavlova, A.; McCarney, E. R.; Peterson, D. W.; Dahlquist, F. W.; Lew, J.; Han, S. *Phys. Chem. Chem. Phys.* **2009**, *11* (31), 6833–6839.
- (18) Yang, J.; Aslimovska, L.; Glaubitz, C. *J. Am. Chem. Soc.* **2011**, *133* (13), 4874–4881.
- (19) Lum, K.; Chandler, D.; Weeks, J. D. *J. Phys. Chem. B* **1999**, *103* (22), 4570–4577.
- (20) Fenimore, P. W.; Frauenfelder, H.; McMahon, B. H.; Parak, F. G. *Proc. Natl. Acad. Sci. U.S.A.* **2002**, *99* (25), 16047–16051.
- (21) Garde, S.; Hummer, G.; Garcia, A. E.; Paulaitis, M. E.; Pratt, L. R. *Phys. Rev. Lett.* **1996**, *77* (24), 4966–4968.
- (22) Russo, D.; Hura, G.; Head-Gordon, T. *Biophys. J.* **2004**, *86* (3), 1852–1862.
- (23) Heugen, U.; Schwaab, G.; Brundermann, E.; Heyden, M.; Yu, X.; Leitner, D. M.; Havenith, M. *Proc. Natl. Acad. Sci. U.S.A.* **2006**, *103* (33), 12301–12306.
- (24) Pethig, R. *Annu. Rev. Phys. Chem.* **1992**, *43*, 177–205.
- (25) Nucci, N. V.; Pometun, M. S.; Wand, A. *J. Nat. Struct. Mol. Biol.* **2011**, *18* (2), 245–U315.
- (26) Modig, K.; Liepinsh, E.; Otting, G.; Halle, B. *J. Am. Chem. Soc.* **2004**, *126* (1), 102–114.
- (27) Persson, E.; Halle, B. *Proc. Natl. Acad. Sci. U.S.A.* **2008**, *105* (17), 6266–6271.
- (28) Zhang, L. Y.; Yang, Y.; Kao, Y. T.; Wang, L. J.; Zhong, D. P. J. *Am. Chem. Soc.* **2009**, *131* (30), 10677–10691.
- (29) Pande, V. S.; Kasson, P. K., P. M.; Lindahl, E. *J. Am. Chem. Soc.* **2011**, *133* (11), 3812–3815.
- (30) Cheng, C. Y.; Wang, J. Y.; Kausik, R.; Lee, K. Y.; Han, S. *J. Magn. Reson.* **2012**, *215*, 115–9.
- (31) Haussler, K. H.; Stehlík, D. *Adv. Magn. Reson.* **1968**, *3*, 79–139.
- (32) Kausik, R.; Han, S. *J. Am. Chem. Soc.* **2009**, *131* (51), 18254–18256.
- (33) Hwang, L. P.; Freed, J. H. *J. Chem. Phys.* **1975**, *63* (9), 4017–4025.
- (34) Kausik, R.; Han, S. *Phys. Chem. Chem. Phys.* **2011**, *13*, 7732–7746.
- (35) Ortony, J. H.; Cheng, C. Y.; Franck, M. J.; Kausik, R.; Pavlova, A.; Hunt, J.; Han, S. *New J. Phys.* **2011**, *13*, 015006.
- (36) Han, S.; McCarney, E. R.; Armstrong, B. D. *Appl. Magn. Reson.* **2008**, *34* (3–4), 439–451.
- (37) Kausik, R.; Srivastava, A.; Korevaar, P. A.; Stucky, G.; Waite, J. H.; Han, S. *Macromolecules* **2009**, *42* (19), 7404–7412.
- (38) Turke, M. T.; Bennati, M. *Phys. Chem. Chem. Phys.* **2011**, *13* (9), 3630–3633.
- (39) Hofer, P.; Parigi, G.; Luchinat, C.; Carl, P.; Guthausen, G.; Reese, M.; Carloni, T.; Griesinger, C.; Bennati, M. *J. Am. Chem. Soc.* **2008**, *130* (11), 3254.
- (40) Sezer, D.; Gafurov, M.; Prandolini, M. J.; Denysenkov, V. P.; Prisner, T. F. *Phys. Chem. Chem. Phys.* **2009**, *11* (31), 6638–6653.
- (41) McCarney, E. R.; Armstrong, B. D.; Kausik, R.; Han, S. *Langmuir* **2008**, *24* (18), 10062–10072.
- (42) Hope, M. J.; Bally, M. B.; Webb, G.; Cullis, P. R. *Biochim. Biophys. Acta* **1985**, *812* (1), 55–65.
- (43) Fukuda, H.; Goto, A.; Yoshioka, H.; Goto, R.; Morigaki, K.; Walde, P. *Langmuir* **2001**, *17* (14), 4223–4231.
- (44) Marsh, D. *Proc. Natl. Acad. Sci. U.S.A.* **2001**, *98* (14), 7777–7782.
- (45) Barre, P.; Eliezer, D. *J. Mol. Biol.* **2006**, *362* (2), 312–326.
- (46) Dalton, L. A.; McIntyre, J. O.; Fleischer, S. *Biochemistry* **1987**, *26* (8), 2117–2130.
- (47) Bennati, M.; Luchinat, C.; Parigi, G.; Turke, M. T. *Phys. Chem. Chem. Phys.* **2010**, *12* (22), 5902–5910.
- (48) Gawrisch, K.; Gaede, H. C.; Mihailescu, M.; White, S. H. *Eur. Biophys. J. Biophys. Lett.* **2007**, *36* (4–5), 281–291.
- (49) Jansen, M.; Blume, A. *Biophys. J.* **1995**, *68* (3), 997–1008.
- (50) Shi, R.; Borgens, R. B. *J. Neurophysiol.* **1999**, *81* (5), 2406–2414.
- (51) Borgens, R. B.; Shi, R. Y.; Bohnert, D. *J. Exp. Biol.* **2002**, *205* (1), 1–12.
- (52) Wang, J.-Y.; Chin, J. M.; Marks, J. D.; Lee, K. Y. C. *Langmuir* **2010**, *26* (15), 12953–12961.
- (53) Firestone, M. A.; Wolf, A. C.; Seifert, S. *Biomacromolecules* **2003**, *4* (6), 1539–1549.